Visualization of aluminum dust flame propagation in a square-section tube: comparison of schlieren, shadowgraphy and direct visualization techniques

Clement Chanut, Frederic Heymes, Pierre Lauret, Zacaria Essaïdi, Pierre Slangen

Visualization of aluminum dust flame propagation in a square-section tube: comparison of schlieren, shadowgraphy and direct visualization techniques

Clement Chanut · Frederic Heymes · Pierre Lauret · Zacaria Essaidi · Pierre Slangen

Abstract This paper presents the results of aluminum dust flame propagation inside a vertical prototype of 700 mm height and 150 × 150 mm square cross section. The study considers three visualization techniques. At first, direct visualization is employed to record the flame light with high speed camera. Special attention is given to collect images without saturation. This is especially important with aluminum flames as they are very luminous. To ensure that the exact delimitation of the flame is well defined, two additional optical techniques have been implemented: schlieren and shadowgraphy. For each explosion test, these three techniques were used simultaneously to compare the flame propagation and the burning velocity. The first one corresponds to the flame speed in the laboratory referential, determined from the obtained images, while the burning velocity corresponds to the consumption rate of the reactants by the flame front. The method used for the determination of burning velocity from the images obtained is exposed. A pulsating behavior of the light emitted by the flame is observed with the direct visualization technique. This behavior confused the determination of the flame front. This contour is easier to define with shadowgraphy images. Nevertheless, results of flame front propagation velocity are close for each technique. Burning velocity is then determined only from direct visualization and shadowgraphy images, to avoid uncertainties due to flame contour detection from schlieren images. Again, results of burning velocity are fairly close for both techniques.

Keywords Flame propagation · Dust explosion · Shadowgraphy · Schlieren · High speed imaging · Burning velocity

1 Introduction

Dust explosion is a major hazard in industries dealing with powders and dusts. All flammable dusts, if fine enough, can cause an explosion when dispersed. Three main categories of combustible powders can be defined: natural organic compounds (corn, carbon, sugar…), synthetic organic compounds (plastics, pigments…) and metallic compounds (aluminum, magnesium…). As a consequence, a lot of industries can be threatened by this hazard, and have to predict the consequences of potential explosions such as thermal effects, overpressure and even projectiles. Models used for gas explosions are sometimes used to predict dust explosion consequences. Although these models seem adapted for organic dusts, they are not accurate enough for metallic ones (Khalili 2012). For this reason, experimental studies are necessary to understand the mechanisms of flame propagation for such explosions. The tricky point of dust explosions experimental investigation is to control the dust concentration and turbulence. Turbulence comes from the injection of

C. Chanut (✉) · F. Heymes · P. Lauret · Z. Essaidi · P. Slangen
LGEI, IMT Mines Ales, University of Montpellier, Ales, France
E-mail: clement.chanut@mines-ales.fr

dust in the test volume before ignition of the cloud (Skjold and Eckhoff 2016). The initial time dependent level of turbulence at ignition has to be known to fully understand the phenomenon (Zhang et al. 2016).

Sensitivity (minimum explosion concentration, minimum ignition energy…) and severity (maximum explosion pressure, maximum rate of pressure rise…) parameters are well-known parameters for risk analysis in the industries. The determination of these parameters is obtained with standardized setups, like the Hartmann tube or the 20 L explosion sphere (Li et al. 2017; Traoré 2007). However, these parameters cannot lead to estimate the explosion power of a given scenario. Numerical simulations have to be performed, requiring others parameters to accurately model the phenomenon. The key parameters are flame velocity, local turbulence, flame wrinkling and thickness. In previous studies, the flame characteristics were analyzed through the visualization of the flame shape over time (Gao et al. 2017). The optical technique mostly used is the direct visualization, which records the light emitted by the flame with a high speed camera. Flames from dust explosions, especially with metallic dusts, are very luminous. So, many images from the literature are saturated, like in Fig. 1 (Ding et al 2010). The flame characteristics can be misestimated with such images, and the resulting interpretation of the flame propagation mechanism possibly wrong. For example, the light emitted by the flame can be diffused by some particles located in front of the flame. This generates uncertainties to define the flame front position

Therefore other optical techniques were tested. Schlieren and shadowgraphy techniques have been used as these are not based on emitted light but on refractive index changes (Settles 2001). These variations are directly linked to temperature (and pressure) variations at the flame front. The first derivative of refractive index is visualized by schlieren technique, whereas the second derivative is obtained by shadowgraphy.

Images of direct visualization, schlieren and shadowgraphy were processed to determine the flame propagation velocity (flame speed in the laboratory referential). However, this velocity depends on the characteristics of the apparatus used. In order to obtain comparable information on the aluminum dust explosion, an independent parameter is used: the burning velocity (consumption rate of the reactants by the flame front). The determination of this velocity requires among other the estimation of the 3D flame surface area. Burning velocity is a key parameter for dust explosion modeling.

2 Materials and methods

2.1 Experimental setup

The prototype has been designed and manufactured for the visualization of aluminum dust flame propagation. The test section is a vertical tube of 700 mm height, with a square cross section of 150 mm × 150 mm. Walls are made out of 10-mm-thick clear glass to allow the visualization of the flame. To disperse the dust, two 1-L compressed air vessels are discharged inside four vertical dust injection tubes, which are located in the corners of the square section tube (Fig. 2). This configuration allows a good homogeneity in terms of concentration along all the prototype height. Mie scattering technique has been used to study and ensure that concentration homogeneity has been reached (Asquini 2019).The aluminum powder under study presents a mean diameter of 6.5 μm.

The ignition of the dust cloud is achieved by a fully characterized electrical spark between two tungsten electrodes, located at the bottom of the prototype. For these experiments, the intensity of the arc is chosen to

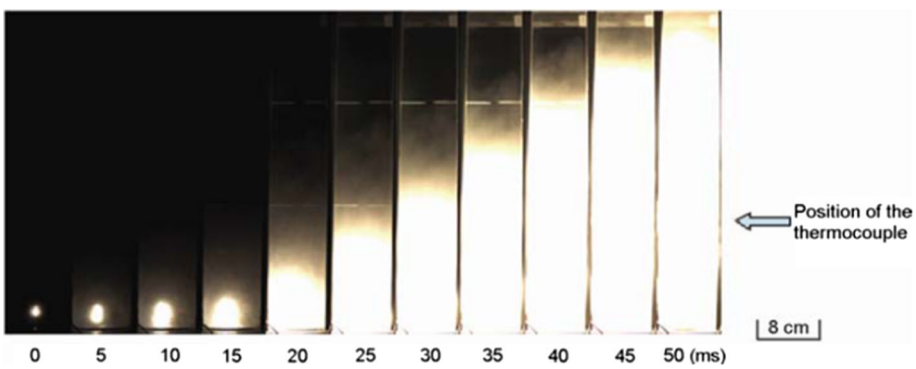

Fig. 1 Saturated images of zirconium dust flame propagation (Ding et al. 2010)

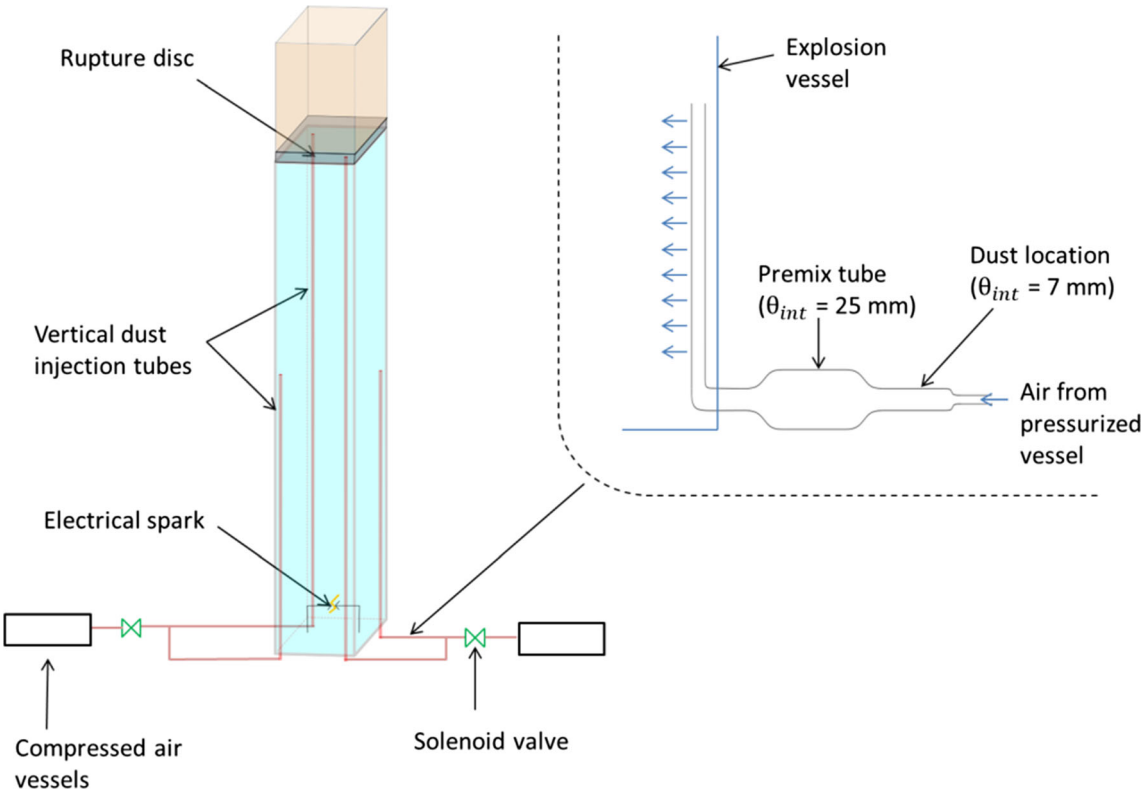

Fig. 2 Experimental apparatus

be 4 A with a duration of 99.9 ms. This yields to the measured energy of about 13 J. This energy E_{spark} is calculated for each test by the measurement of intensity (I) and voltage (U) across the electrodes:

$$E_{\text{spark}} = \int U(t) \cdot I(t) \cdot \mathrm{d}t \tag{1}$$

A rupture disc is located at the top of the prototype. The aim is to limit the overpressure inside the prototype but also to keep control on the dust concentration. Finally above the disc, the flow is conducted through an outlet tube.

The experimental protocol is as follows. First, dust is weighted and placed inside the injection tubes. Both air vessels are pressurized up to 2.5 bar. Then, the solenoid valves are opened during 0.8 s. Another 0.75 s after closing the valves, dust cloud is ignited by the electrical spark. The turbulence intensity at the moment of ignition is about 34 cm/s (Asquini 2019). This value has been determined with particle image velocimetry (PIV) and laser Doppler anemometry (LDA) techniques. For these tests, the aluminum concentration is around 350 g m^{-3}. This concentration is determined by measuring the weight of the dust inside each injection tube before and after each test.

Details of the experimental setup and of the optical methods used for dust cloud characterization (concentration homogeneity and turbulence) can be found in (Asquini 2019).

2.2 Optical configuration

For each test, flame propagation was simultaneously recorded by the three optical techniques (Fig. 3). Two zones of interest have been studied: from the bottom of the tube up to 30 cm and between 20 and 50 cm in height. Although several tests were realized for each zone of interest, only one representative result obtained for each zone is exposed.

For direct visualization, Vision Research Phantom V2512 high-speed camera was used, with a 70–200 mm lens. For our setup, the maximal resolution was kept by 1280 × 800 pixels with the widest side along the vertical axis. The acquisition frequency was lowered to 7500 fps to cope with other cameras. Lens

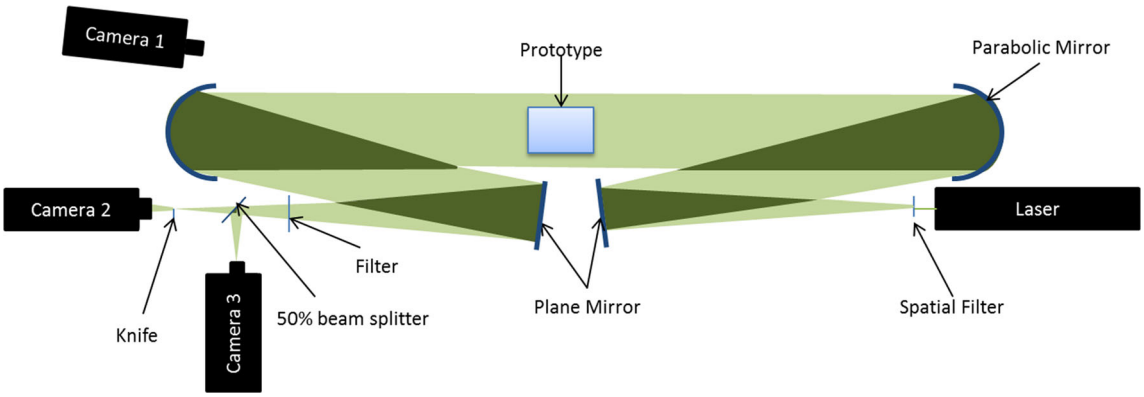

Fig. 3 Optical setup

aperture was f/32 to give larger depth of field and mostly to reduce the saturation. Exposure time was set to 5 µs, with 2.5 µs extreme dynamic range (EDR), for the images obtained in the lower part of the prototype. For the upper part of the prototype, the exposure time is set to 2 µs, with 1 µs EDR. EDR enables to dynamically change the pixel saturation from one image to the next one and so to optimize the dynamic range of the region of interest presenting deep changes of light intensity distribution. With these parameters, non-saturated images are obtained during all the flame propagation. It is especially important to analyze non-saturated images for the determination of the burning velocity (Chanut et al. 2018).

For schlieren and shadowgraphy techniques, specific light source passing through the prototype was mandatory. However, this light source can be tremendously attenuated by the dust located inside the tube before ignition. Besides, as aluminum flames are very luminous, camera sensor will be saturated by the flame light, or not sensitive to the assigned light source (depending on the exposure camera settings). To avoid this limitation, a powerful laser has been used, coupled with band-pass interferential filter to deeply attenuate the light emitted by the flame. The laser source is a 5 W Coherent VERDI laser emitting at the wavelength of 532 nm. The laser beam is expanded by a spatial filter made of 20X microscope objective couple to 10 µm pinhole to reach homogeneous Gaussian beam. The size of the region of interest is fixed by the 30 cm diameter parabolic mirrors. The Z-setup requires two 254 cm focal length f/8 parabolic mirrors (Edmunds Optics, enhanced aluminum) to reach good sensitivity. Band pass filter and 50% beam splitter are placed before the conjugate image of the spatial filter spot. This generates two identically balanced beams, only sensitive to the dedicated laser source. Knife edge placed on the source image spot produces the schlieren filtering. Schlieren enables refractive index variations along one axis to be visualized, in our case the vertical axis. Vision Research Phantom V711 high-speed camera gives 7.6 GB/s throughput for the schlieren arm. Exposure time is 5 µs, with 2.5 µs EDR. The resolution is 1280 × 800 pixels with the maximum 7500 fps frequency. It is mounted with a Tamron 30–700 mm lens. Lens aperture is f/4. Finally, for shadowgraphy, another Vision Research Phantom V2512 high-speed camera is used with the same optical and recording parameters as for schlieren visualization. All these optical parameters are summarized in Table 1.

2.3 Analysis method

Flame contour is estimated from the images obtained with an algorithm based on Canny method and on thresholding (Canny 1986). The determination of the flame contour is somewhat arbitrary because of the choice of some parameters for the algorithm. From this contour, the flame front position can be determined. It corresponds to the higher point of the flame front contour. Then, the propagation velocity is evaluated.

Table 1 Summary of optical parameters

Optical technique	Camera	Frequency (fps)	Resolution (px)	Exposure time (EDR)	Lens (mm)	Lens aperture
Direct visualization	V2512	7500	1280 × 800	2 µs (1 µs): upper part 5 µs (2.5 µs): lower part	70–200	f/32
Shadowgraphy	V2512	7500	1280 × 800	5 µs (2.5 µs)	70–300	f/4
Schlieren	V711	7500	1280 × 800	5 µs (2.5 µs)	70–300	f/4

The flame propagation velocity(V_p) is the flame speed in the laboratory referential. The burning velocity is evaluated in two main steps from this velocity. This method is based on the work of Andrews and Bradley (1972) and has been already used for dust flame propagation analysis in previous studies (Cuervo 2015; Di Benedetto et al. 2011).

The first step takes into account for the thermal expansion of the burned gases. Because the flame propagates from the close bottom end to the open top end of the prototype, propagation velocity is higher than burning velocity. Thus, a first burning velocity (S'_u) can be defined as follows:

$$Su' = \frac{V_p}{\chi} \tag{2}$$

where χ is the thermal expansion coefficient, calculated as follows:

$$\chi = \frac{\rho_u}{\rho_b} \approx \frac{T_b}{Tu} \tag{3}$$

where ρ_u and ρ_b are the densities of the unburned and burned gases, respectively. T_u and T_b are the unburned gases temperature (ambient temperature) and the flame temperature (supposed adiabatic).

This adiabatic flame temperature is calculated with the Chemical Equilibrium with Applications (CEA) software (Gordon and McBride 1994). This flame temperature, calculated with the test conditions T = 3092 K, leads to a thermal expansion coefficient around 10.5.

The second step takes into account for the non-planar shape of the flame front. The burning velocity (S_u) is defined as the propagation velocity of a planar flame. However, because of instabilities, a planar flame is unstable. The burning velocity (S_u) is then determined as follows from the previous burning velocity (S'_u):

$$Su = \frac{A'}{A_f} \times Su' \tag{4}$$

where A' is the projected flame surface area on a horizontal plane and A_f is the 3D flame surface area.

One major difficulty of this method is the estimation of the 3D flame surface area from 2D images of the flame front. Figure 4 presents the Khalili's method (2012) for this estimation from the recorded images. In this method, the flame profile is approximated by ellipses on the plane perpendicular to the viewed plane. The procedure is as follows: first, the flame front contour is determined from the images. Then, a circle is traced at the bottom of the flame contour on a horizontal plane. Then the unique ellipses are traced between the circle and each point of the flame profile. From this 3D surface estimation, the 3D area of the flame front can then be evaluated.

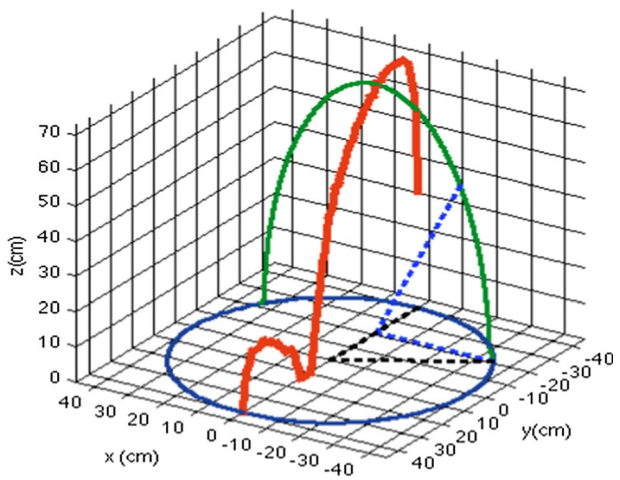

Fig. 4 Methodology of flame surface area estimation, from Khalili (2012). Red line: detected flame contour. Green line: approximate flame contour

3 Results

3.1 Visualization of the propagation

Figures 5 and 6 present the images of the flame front propagation, respectively, in the lower zone and in the upper zone of visualization. In each figure, the images obtained with each visualization technique are presented. Images of direct visualization obtained are not saturated. As cameras are recording 12 bits pixels, the raw images are not saturated, but bitshift can be applied to the pixel dynamic range to cope with 8 bits display. These images of direct visualization show a pulsating behavior of their luminosity. Julien et al. (2015) also observed this behavior during aluminum flame propagation in a balloon. The contour of the flame is difficult to detect because of this behavior. Indeed, in some images the flame front is almost invisible (Fig. 6a, t = 207.3 ms), whereas in others the flame is very luminous (Fig. 6a, t = 179.3 ms).

With schlieren technique, the shape of the flame front during the 3D propagation around the electrodes is not visible. This technique allows the visualization of the refractive index variations only along the vertical axis. For this reason, details of the flame front are also less visible during 1D propagation. This has been selected on purpose to show the vertical change of refractive index and not the horizontal one.

With shadowgraphy, more details of the flame front structure are visible, and the flame contour seems easier to define. Besides, the flame front is always detectable even when it is almost invisible by direct visualization.

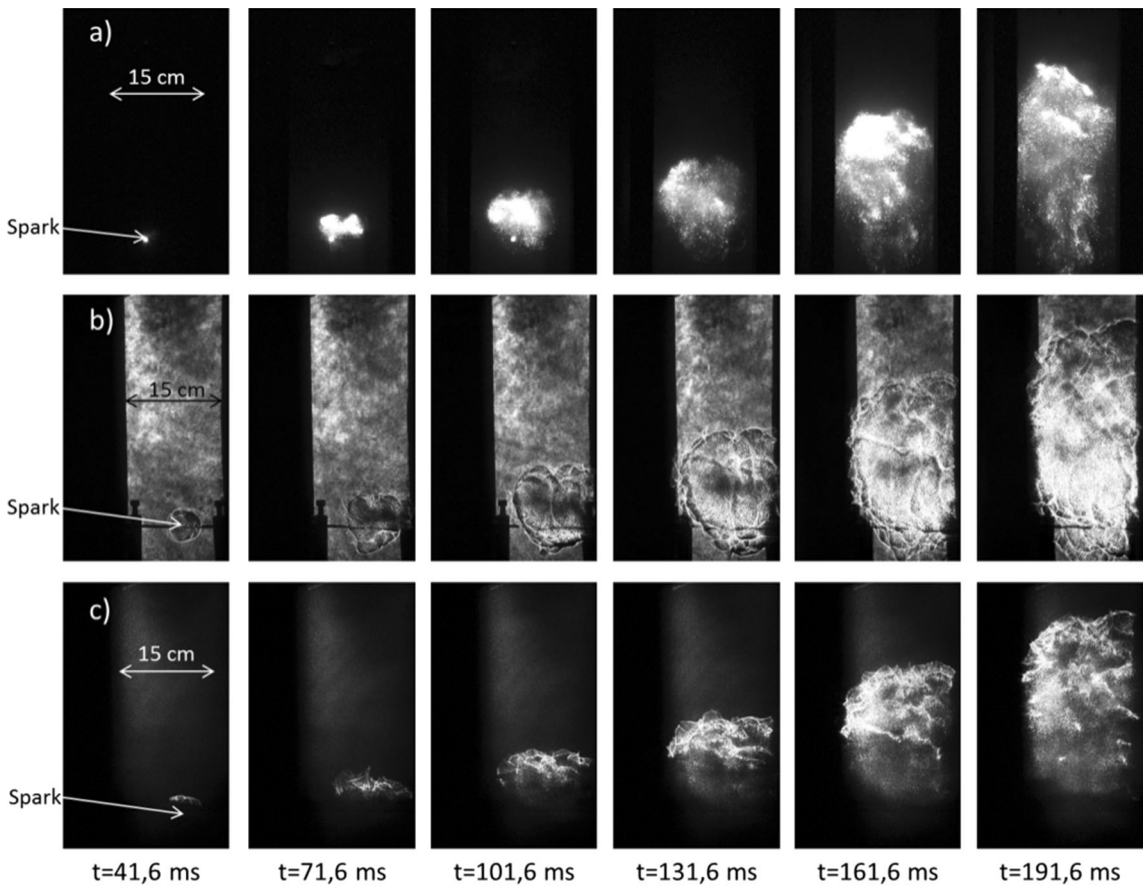

Fig. 5 Flame propagation visualization on the lower part of the prototype: by direct visualization (**a**), shadowgraphy (**b**) and schlieren (**c**). Time between images: 30 ms

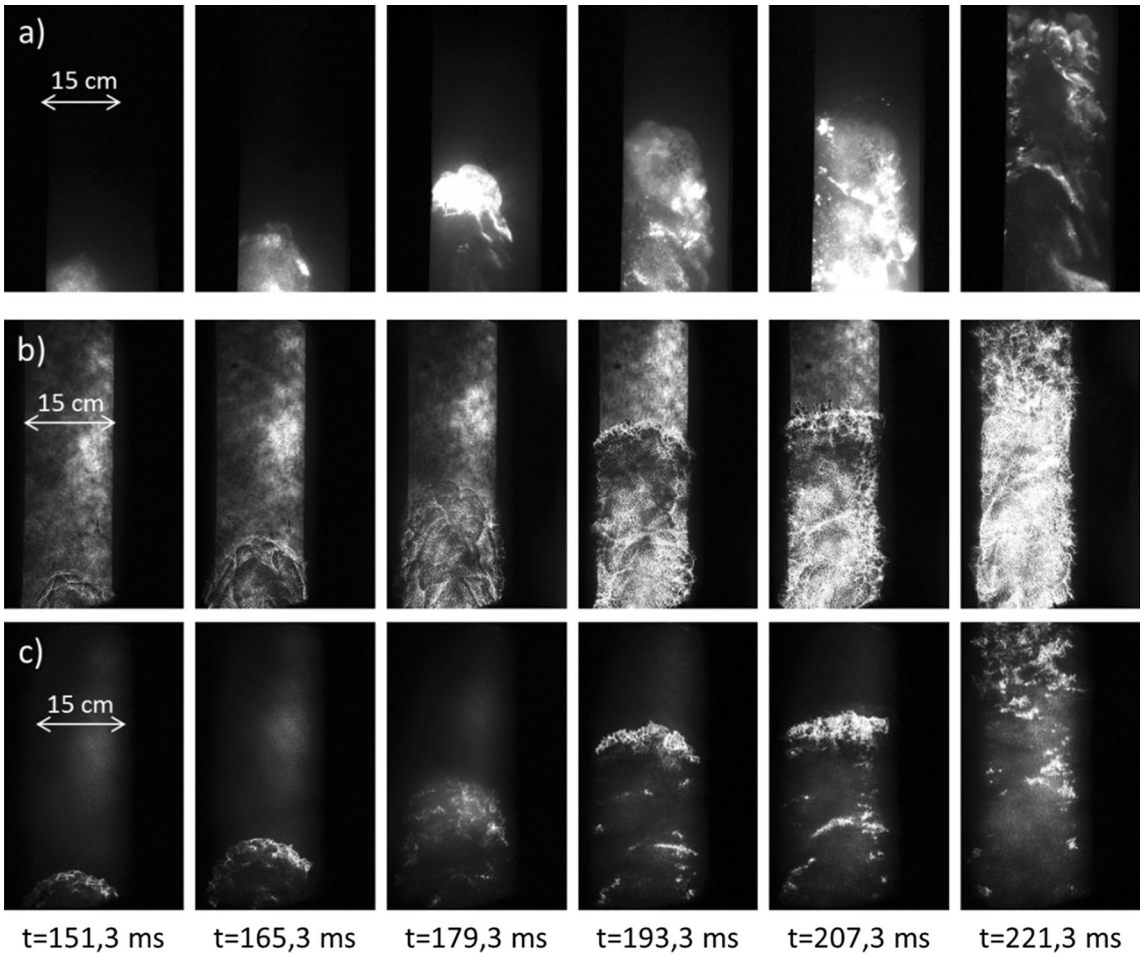

Fig. 6 Flame propagation velocity on the upper part of the prototype: by direct visualization (**a**), shadowgraphy (**b**) and schlieren (**c**). Time between images: 14 ms

3.2 Determination of the propagation velocity

Figure 7 presents the evolution of the flame front position over time, obtained with each visualization technique. The flame propagation can be divided in four stages, depending on its velocity and its light intensity. Indeed, on the right of Fig. 7, the evolution of the flame light intensity is compared to the evolution of the flame front propagation. This light intensity estimation is the spatial mean (over all the images) of the pixel values of each image obtained by the direct visualization technique. This qualitative estimation of light intensity fluctuations is just used to show the trends between light intensity and velocity fluctuations.

First, the flame propagates slowly, with a fairly constant acceleration. Suddenly, flame strongly accelerates and becomes very luminous. Then, the flame decelerates until reaching a null velocity. At this time, the flame front is quite invisible with direct visualization while with shadowgraphy it looks planar and propagates downward. Finally, the flame reaccelerates, becoming very luminous again. This light intensity behavior is in accordance with previous results of Julien et al. (2015).

Flame position is always lower with direct visualization than with shadowgraphy or schlieren. It seems logical because with the first technique the luminous front is detected, which is linked to the combustion zone, whereas with shadowgraphy and schlieren, the temperature gradient is observable, which corresponds to the pre-heating zone. So, the difference of flame front position should be close to the value of flame thickness. However, in our result, this difference seems too important to correspond to the flame front thickness. This difference can also be explained by the difficulties to define the flame front position with direct visualization images.

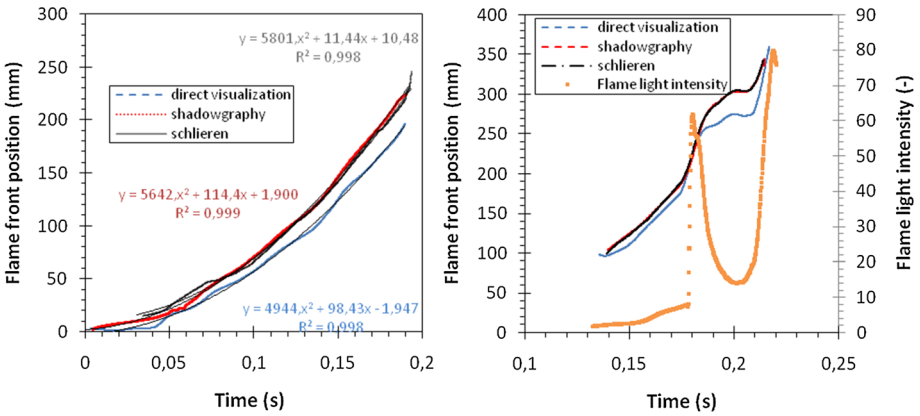

Fig. 7 Evolution of the flame front position with each techniques: for the lower zone (left) and the upper zone (right) of visualization

Figure 8 presents the evolution of the propagation velocity obtained from the flame front position data (temporal derivative). In the lower part (Fig. 8 left), the flame does not propagate with a constant acceleration. A pulsating behavior is observed, with some accelerations and decelerations. In the upper part of the prototype (Fig. 8 right), fast acceleration of the flame is observed, with a flame velocity up to 8 m/s. The shape of the propagation velocity curve is similar for each visualization techniques. The differences can be due to difficulties to define the flame front contour.

3.3 Estimation of the burning velocity

From the flame front contour obtained, the burning velocity is determined with the method previously presented. First, the flame front surface area has to be determined. The determination of this surface has been obtained only with the images from direct visualization and shadowgraphy, because the flame front contour was too difficult to define with schlieren images as above-mentioned. With both techniques the flame burning velocity has the same behavior and similar values (Fig. 9).

A unique burning velocity is difficult to define because of the acceleration of the flame (pulsating behavior). This behavior is linked to the aluminum concentration (Julien et al. 2015). This propagation will then be studied in a longer prototype (about 2 m long) to see whether the flame presents a stable behavior over larger distances.

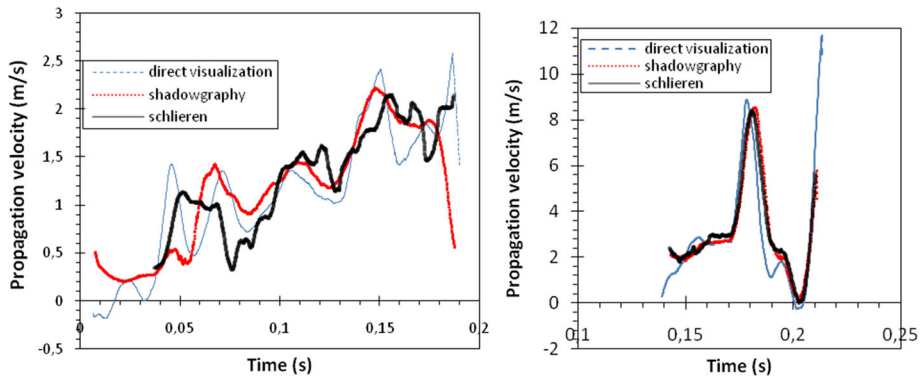

Fig. 8 Evolution of the propagation velocity with each techniques: for the lower zone (left) and the upper zone (right) of visualization

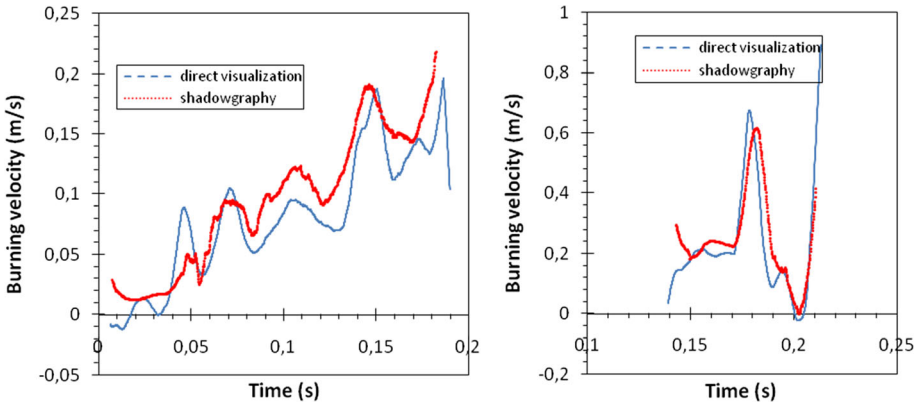

Fig. 9 Evolution of the burning velocity with direct visualization and shadowgraphy: for the lower zone (left) and the upper zone (right) of visualization

4 Conclusion

Aluminum dust flame propagation in a tube has been visualized by three optical techniques: direct visualization, schlieren and shadowgraphy. With the images obtained with each technique, the flame front propagation has been determined and compared. However, the burning velocity has been computed only from direct visualization and shadowgraphy images because the definition of the flame surface area with schlieren technique is too weak. The results of velocities obtained with the compared techniques are fairly close.

With schlieren, the flame front surface is difficult to detect, especially during the 3D propagation, around the electrodes. With direct visualization, some flame characteristics can be observed, as the pulsating behavior. However, the flame front is sometimes difficult to detect because light intensity oscillates together with flame velocity. In some images the flame front is almost invisible, whereas it is very luminous at other times. Moreover, the flame front definition is somewhat arbitrary with this optical technique; especially in case of saturated images obtained by direct visualization (Chanut et al. 2018). Shadowgraphy seems the best technique to detect the flame front. There is less luminosity variation during the propagation than with direct visualization. Moreover, some details of the flame front are more visible with this technique than with schlieren, due to one-axis orientation of schlieren.

The main objective of this study was to check the accuracy of the methods used to determine the burning velocity during dust explosion in tubes. In this field, direct visualization is mainly used. Previously, the authors pointed that non-saturated images should be used (Chanut et al. 2018). With non-saturated images, the estimation of burning velocity by shadowgraph or by direct visualization is fairly close. Even if shadowgraph is widely used for gas explosion, this technique is less used for dust explosions because of the difficulty to implement it (very luminous flame, presence of particles…); indeed for these tests a powerful laser source had to be used. Using the direct visualization technique, researchers have to be careful on the behavior of the flame front: because of saturation and pulsating behavior.

One major difficulty with the determination of the burning velocity is the evaluation of the 3D flame surface area from 2D images. In our analysis, the latter is estimated with a method based on ellipse. Another method to be compared to this one would be based on visualization of the flow in front of the flame front by particle image velocimetry (PIV). With PIV, the fresh mixture velocity can be determined and compared to the flame propagation velocity. Then, with the difference of both velocities, the burning velocity can be calculated. This technique will also allow the determination of the burning velocity locally (Proust 2006).

Acknowledgements The authors are grateful to IRSN (Institut de Radioprotection et Surete Nucleaire) for the scientific and financial support of this research project.

References

Andrews GE, Bradley D (1972) Determination of burning velocities: a critical review. Combust Flame 18:133–153

Asquini E (2019) Influence of turbulence on flame propagation during dust explosions. Dissertation. https://doi.org/10.5281/zenodo.3706671
Canny J (1986) A computational approach to edge detection. IEEE Trans Pattern Anal Mach Intell 8:679–698
Chanut C, Heymes F, Lauret P, Slangen P (2018) Visualization of aluminum dust flame propagation in a square-section tube. Chem Eng Trans 67:7–12. https://doi.org/10.3303/CET1867002
Cuervo N (2015) Influences of turbulence and combustion regimes on explosions of gas-dust hydrid mixtures. Dissertation, Université de Lorraine
Di Benedetto, A, Garcia-Agreda, A, Dufaud, O, Khalili, I, Sanchirico, R, Cuervo, N, Perrin, L, Russo, P (2011) Flame propagation of dust and gas-air mixtures in a tube. In: MCS7 seventh mediterranean combustion symposium, pp 11–13
Ding Y, Sun J, He X, Wang Q, Yin Y, Xu Y, Chen X (2010) Flame propagation characteristics and flame structures of zirconium particle cloud in a small-scale chamber. Chin Sci Bull 55:3954–3959
Gao W, Zhang X, Zhang D, Peng Q, Zhang Q, Dobashi R (2017) Flame propagation behaviours in nano-metal dust explosions. Powder Technol 321:154–162. https://doi.org/10.1016/j.powtec.2017.08.013
Gordon, S, McBride, BJ (1994) Computer program for calculation of complex chemical equilibrium compositions and applications. NASA RP 1311
Julien P, Vickery J, Goroshin S, Frost DL, Bergthorson JM (2015) Freely-propagating flames in aluminum dust clouds. Combust Flame 162:4241–4253. https://doi.org/10.1016/j.combustflame.2015.07.046
Khalili I (2012) Sensibilité, sévérité et spécificités des explosions de mélanges hybrides gaz/vapeurs/poussières. Dissertation, Université de Lorraine
Li Y, Liu F, Zhang Q, Yu Y, Shu CM, Jiang J (2017) Explosion characteristics of micron-size conveyo rubber dust. J Loss Prev Process Ind 45:173–181. https://doi.org/10.1016/j.jlp.2016.12.005
Proust C (2006) Flame propagation and combustion in some dust-air mixtures. J Loss Prev Process Ind 19:89–100. https://doi.org/10.1016/j.jlp.2005.06.026
Settles GS (2001) Schlieren and shadowgraph techniques. Experimental fluid mechanics. Springer, Berlin, Heidelberg
Skjold T, Eckhoff RK (2016) Dust explosions in the process industries: research in the twenty-first century. Chem Eng Trans 48:337–342
Traoré M (2007). Explosion de poussières et de mélanges hybrides. Etude paramétrique et relation entre la cinétique de combustion et la violence de l'explosion. Dissertation, Institut National Polytechnique de Lorriane
Zhang X, Yu J, Sun J, Gao W (2016) Effects of turbulent intensity on nano-PMMA flame propagation behaviors. J Loss Prev Process Ind 44:119–124. https://doi.org/10.1016/j.jlp.2016.09.001